Published in final edited form as:
Dev Dyn. 2008 December ; 237(12): 3809–3819. doi:10.1002/dvdy.21803.

Cooperative interaction of *Nkx2.5* and *Mef2c* transcription factors during heart development

Joshua W. Vincentz, **Ralston M. Barnes**, **Beth A. Firulli**, **Simon J. Conway**, and **Anthony B. Firulli***
Riley Heart Research Center, Herman B Wells Center for Pediatric Research Division of Pediatrics Cardiology, Departments Anatomy and Medical and Molecular Genetics, Indiana Medical School, 1044 W. Walnut St., Indianapolis, IN 46202−5225, USA

Abstract

The interactions of diverse transcription factors mediate the molecular programs that regulate mammalian heart development. Among these, *Nkx2.5* and the *Mef2c* regulate common downstream targets and exhibit striking phenotypic similarities when disrupted, suggesting a potential interaction during heart development. Co-immunoprecipitation and mammalian two-hybrid experiments revealed a direct molecular interaction between Nkx2.5 and Mef2c. Assessment of mRNA expression verified spatiotemporal cardiac coexpression. Finally, genetic interaction studies employing histological and molecular analyses showed that, although *Nkx2.5*$^{-/-}$ and *Mef2c*$^{-/-}$ individual mutants both have identifiable ventricles, *Nkx2.5*$^{-/-}$;*Mef2c*$^{-/-}$ double mutants do not, and that mutant cardiomyocytes express only atrial and second heart field markers. Molecular marker and cell death and proliferation analyses provide evidence that ventricular hypoplasia is the result of defective ventricular cell differentiation. Collectively, these data support a hypothesis where physical, functional and genetic interactions between Nkx2.5 and Mef2c are necessary for ventricle formation.

Keywords

Nkx2.5; *Mef2c*; heart development; ventricle; mouse

Introduction

Formation of the mammalian heart requires the differentiation of mesodermal and ectomesenchymal cell populations and subsequent integration of these cells into a functioning organ. Precise transcriptional control of morphogenic patterning and cell differentiation is central to the implementation of this collective cardiogenic program. Extensive transgenic studies have elegantly established the unique requirements of a number of individual transcription factors for normal cardiogenesis in the mouse. However, the degree to which interaction of these multiple factors coordinate specific aspects of heart development is only now beginning to be resolved.

The primitive linear heart tube, constituting the primary heart field (PHF), is segmentally patterned along a rostral-caudal axis in a manner that establishes progenitors of the ventricles, atria and sinus venosus (Sucov, 1998; Srivastava, 2001). A distinct population, termed the secondary heart field (SHF), is progressively added to the outflow and inflow regions of the heart during looping (Kelly et al., 2001; Mjaatvedt et al., 2001; Waldo et al.,

* Corresponding Author Fax: 317−278−5413 Email tfirulli@iupui.edu.

2001; Cai et al., 2003). Subsequent to these initial cell specifications, each segment undergoes unique proliferation and differentiation programs that culminate in the formation of the specialized components of the functional heart. During development, large number of transcription factors ultimately regulate the development of the heart (Firulli and Thattaliyath, 2002). Two of these factors, the NK-class homeobox transcription factor *Nkx2.5* and the MADs box transcription factor *Mef2c* have been shown to be key regulators of cardiac development.

Both *Nkx2.5* and *Mef2c* are expressed during early cardiogenesis (Lints et al., 1993; Edmondson et al., 1994). Growth of *Nkx2.5*$^{-/-}$ mutant hearts arrests during looping. These hearts present a single ventricular chamber, which can be identified by the expression of *Mlc2v*, a reduction of myocardial trabeculation, and an under-developed outflow tract (Lyons et al., 1995; Tanaka et al., 1999). Similarly, ablation of *Mef2c* gene function causes cardiac growth arrest during looping, formation of a single *Mlc2v*-expressing ventricular chamber, defective myocardial trabeculation, and a delay of cell differentiation in the outflow tract (Lin et al., 1997; Vong et al., 2006).

Importantly, both Nkx2.5 and Mef2c can each homodimerize (Molkentin et al., 1996; Kasahara et al., 2001), bind DNA, and regulate common cardiac-specific genes such as *ANF* (*Nppa*; (Durocher et al., 1996; Zang et al., 2004). Additionally, both factors interact and cooperatively regulate transcription with other critical cardiac transcription factors, such as Hand2 and Gata4 (Durocher et al., 1997; Morin et al., 2000; Yamagishi et al., 2001; Vanpoucke et al., 2004; Zang et al., 2004) Significantly, Nkx2.5 and Mef2c have been shown to participate in a positive transcriptional feedback loop which initiates cardiomyogenesis (Skerjanc et al., 1998). Given these phenotypic and functional commonalities, we hypothesized that Nkx2.5 and Mef2c cooperate to regulate aspects of the cardiac program.

Here, we employ co-immunoprecipitation experiments and mammalian 2-hybrid analyses to demonstrate that Nkx2.5 and Mef2c molecularly interact *in vivo*, and provide evidence that these interactions modulate homodimer formation. Additionally, we histologically and molecularly assess the cardiac phenotype of *Nkx2.5*$^{-/-}$;*Mef2c*$^{-/-}$ compound mutant embryos, finding that, although both *Nkx2.5*$^{-/-}$ and *Mef2c*$^{-/-}$ individual mutants have morphologically and molecularly identifiable ventricles, *Nkx2.5*$^{-/-}$;*Mef2c*$^{-/-}$ double mutants display ventricular hypoplasia, a more severe cardiac phenotype than those associated with either single mutant. Assessment of ventricular markers, cell death, and cell proliferation suggests that this genetic interaction reflects a defect of cell specification. Collectively, these data define a functional role of genetic Nkx2.5 and Mef2c interactions during cardiovascular development.

Results

Characterization of molecular interactions between Nkx2.5 and Mef2c

As both Nkx2.5 and Mef2c are known to interact with common cardiac transcription factors, such as Hand2 and Gata4, and both factors commonly transcriptionally regulate similar downstream targets, we first sought to establish whether there is direct molecular interaction between Nkk2.5 and Mef2c. To this end, we performed co-immunoprecipitation experiments. N-terminal Myc epitope-tagged Nkx2.5 and Mef2c were co-expressed with FLAG-tagged Mef2c in HEK293 cells. Mef2c forms a homodimer (Molkentin et al., 1996), and as expected, immunoprecipitation of FLAG-tagged Mef2c pulled down coexpressed Myc-tagged Mef2c (Fig. 1A). We also consistently observed a Myc-tagged species of lower molecular weight that is most likely a Mef2c breakdown product. Significantly, FLAG-tagged Mef2c also pulled down Myc-tagged Nkx2.5, indicating a protein-protein interaction

(Fig. 1A). Similarly, when FLAG-tagged Nkx2.5 was employed in immunoprecipitation analysis, Nkx2.5 homodimers were readily detectable (Fig. 1B). FLAG-tagged Nkx2.5 could also pull down Myc-tagged Mef2c, as well as the observed undetermined breakdown product, albeit at very low levels (Fig. 1B).

To further explore the nature of these Nkx2.5/Mef2c interactions, we performed mammalian 2-hybrid assays. The mammalian 2-hybrid assay identifies interactions between two proteins of interest via fusion of these proteins to either a GAL4 DNA-binding domain (the pBIND construct) or VP16 transcriptional activation domain (the pACT construct), respectively. Juxtaposition of these GAL4 and VP16 domains via direct protein-protein interaction enables upregulation of a luciferase reporter cassette (Firulli et al., 2000). Contrasting with the aforementioned immunoprecipitation results, initial experiments employing pACT-Nkx2.5 and pBIND-Mef2c, or pACT-Mef2c and pBIND-Nkx2.5 fusion proteins failed to show a direct interaction between Mef2c and Nkx2.5. Thus, although Nkx2.5 and Mef2c could each homodimerize; they did not interact as heterodimers in this experimental context (Fig. 1C). Interestingly, coexpression of Mef2c with both Nkx2.5 GAL4 and VP16 fusion proteins revealed that Mef2c enhanced formation of the Nkx2.5 dimer (Fig. 1D). Conversely, coexpression of Nkx2.5 with Mef2c GAL4 and VP16 fusion proteins showed that Nkx2.5 disrupted formation of the Mef2c dimer, as indicated by the drop in luciferase activity when compared to Mef2c homodimer strength in the absence of Nkx2.5 (Fig. 1E). Further 2-hybrid analyses showed that Nkx2.5 inhibition of Mef2c homodimerization and Mef2c stabilization of Nkx2.5 homodimer formation is dose-dependant (Fig. 1F, G).

To validate these results, we performed additional co-immunoprecipitation experiments to assess the respective ability of increasing concentrations of Nkx2.5 and Mef2c to reciprocally modulate each other's homodimerization potential. To this end, FLAG and Myc epitope-tagged Nkx2.5 fusion proteins were co-expressed in HEK293 cells in the presence of increasing concentrations of Myc-tagged Mef2c. Immunoprecipitation of FLAG-tagged Nkx2.5 pulled down progressively greater quantities of Myc-tagged Nkx2.5 as Mef2c levels were increased (Fig. 1H). These results are consistent with mammalian 2-hybrid results indicating that Mef2c stabilizes Nkx2.5 homodimerization. No difference in the ability of FLAG-tagged Mef2c to pull down Myc-tagged Mef2c in the presence of increasing levels of Nkx2.5 was observed (data not shown). In our hands, Mef2c homodimerization is comparatively more readily detectable than Nkx2.5 homodimerization in co-immunoprecipitation experiments. Given the strength of Mef2c homodimerization in these assays, potential homodimer destabilization may be below their sensitivity.

As a whole, these data demonstrate that Nkx2.5 and Mef2c molecularly interact in a non-canonical manner, that is, in a way that influences homodimer formation, rather than direct formation of a heterogenic molecular complex.

Expression of Nkx2.5 and Mef2c in wild-type and mutant hearts

Nkx2.5 and *Mef2c* are expressed in restricted domains within the developing heart (Komuro and Izumo, 1993; Lints et al., 1993; Edmondson et al., 1994). We sought to investigate the physiological relevance of the physical interactions seen between Nkx2.5 and Mef2c in our *in vitro* experiments by first identifying tissues in which these two factors are coexpressed. To this end, we performed DIG-labeled *in situ* hybridization analyses upon adjacent sagittal sections of E8.5 (7−11 somite stage) embryos. During the early stages of heart looping, *Mef2c* is broadly expressed in the atria, ventricles, and outflow tract (Fig. 2A). *Nkx2.5* is even more broadly expressed, and is detectable in the foregut endoderm (Fig. 2B). These respective expression domains completely overlapped with that of the early and specific marker of ventricular cardiomyocytes, *Myosin light chain 2v* (*Mlc2v*: Fig. 2C). Thus, *Mef2c*

and *Nkx2.5* are broadly coexpressed in the developing heart, including a domain completely overlapping that of the developing ventricle.

Nkx2.5 expression is unaffected in *Mef2c*$^{-/-}$ mutants (Lin et al., 1997). However, *Mef2c* expression is downregulated in E9.5 *Nkx2.5*$^{-/-}$ mutant hearts (Tanaka et al., 1999). If Nkx2.5 is a regulator of *Mef2c* expression, and the phenotypic similarities shared by *Mef2c*$^{-/-}$ and *Nkx2.5*$^{-/-}$ embryos may reflect a phenocopy. To investigate the regulatory relationship between *Mef2c* and *Nkx2.5* more completely, we sought to define this relationship at an earlier developmental stage. *In situ* hybridization analyses at E8.5 (7−13 somite stage) revealed that, as expected, *Nkx2.5* is robustly expressed in *Mef2c*$^{-/-}$ mutant hearts (Fig. 2E). Surprisingly, *Mef2c* is also robustly expressed in *Nkx2.5*$^{-/-}$ mutants at this stage, (Fig. 2D). These data indicate that a loss of *Nkx2.5* may cause a gradual diminution of cardiac *Mef2c* expression, but does not affect initial *Mef2c* upregulation. These two genes thus occupy parallel developmental pathways.

Histological and molecular characterization of genetic interactions between Nkx2.5 and Mef2c

To assess potential genetic interaction between *Nkk2.5* and *Mef2c*, we intercrossed *Nkx2.5*$^{+/-}$;*Mef2c*$^{+/-}$ mice, then histologically and molecularly examined resulting embryos. Analyses of E9.5 embryos show that, as previously reported, *Nkx2.5*$^{-/-}$ and *Mef2c*$^{-/-}$ single mutant embryos display cardiac defects, including growth arrest during looping, but have morphologically identifiable atria and ventricles (Fig. 3D-I). *Nkx2.5*$^{+/-}$;*Mef2c*$^{-/-}$ and *Nkx2.5*$^{-/-}$;*Mef2c*$^{+/-}$ embryos were phenotypically indistinguishable from *Mef2c*$^{-/-}$ and *Nkx2.5*$^{-/-}$ single mutants, respectively. In contrast, *Nkx2.5*$^{-/-}$;*Mef2c*$^{-/-}$ embryos showed no evidence of cardiac looping, and exhibit a single morphologically identifiable heart chamber (h) and a hypoplastic outflow tract (arrowhead, Fig. 3J-L).

Nkx2.5$^{-/-}$;*Mef2c*$^{-/-}$ embryos were subsequently sectioned and stained with H&E. These sections confirm the presence of a single heart chamber within the double null embryos (Fig. 4K). Further analyses revealed extremely dilated sinus venosus in *Nkx2.5*$^{-/-}$;*Mef2c*$^{-/-}$ embryos, a phenotype associated with impaired cardiac function (Fig. 4L). Examination of outflow tracts of *Nkx2.5*$^{-/-}$ and *Mef2c*$^{-/-}$ single mutants revealed that, although *Nkx2.5*$^{-/-}$ mutants fail to form atrioventricular cushions, identifiable outflow tract cushions are apparent in both single mutants. *Nkx2.5*$^{-/-}$;*Mef2c*$^{-/-}$ embryos, however, display an almost total lack of outflow tract cushions. Indeed, the outflow tract canal is extremely narrow in *Nkx2.5*$^{-/-}$;*Mef2c*$^{-/-}$ embryos (Fig. 4K), no doubt impeding circulation and potentially accounting for the dilation of the sinus venosus mentioned above. Additionally, the caudal pharyngeal arches of *Nkx2.5*$^{-/-}$;*Mef2c*$^{-/-}$ mutants are hypoplastic, although this phenotype is also observed in single *Mef2c*$^{-/-}$ hearts (asterisks in Fig. 4G and 4J).

Although the hearts in *Nkx2.5*$^{-/-}$;*Mef2c*$^{-/-}$ double mutants were grossly morphologically distinct from either *Nkx2.5*$^{-/-}$ or *Mef2c*$^{-/-}$ single mutants, it was unclear whether this distinction reflected aberrant morphogenesis or wholesale tissue loss. *Nkx2.5*$^{-/-}$;*Mef2c*$^{-/-}$ hearts, although unlooped, superficially appeared wider than the partially looped hearts of *Nkx2.5*$^{-/-}$ and *Mef2c*$^{-/-}$ single mutants (Fig. 3L). We therefore performed morphometric analyses to assess the total relative volume of the cardiomyocytes in these embryos. To this end, we isolated the photographic area occupied by the cardiomyocytes and quantified the number of pixels comprising the isolated tissues. To account for variation in cardiac volume due to hearts being in ether systole or diastole when fixed, only cardiomyocyte area, not that of the cardiac lumen or sinus venosus, was measured for these assays. These results show that *Nkx2.5*$^{-/-}$, *Mef2c*$^{-/-}$ and *Nkx2.5*$^{-/-}$;*Mef2c*$^{-/-}$ mutants all have a diminished cardiomyocyte volume relative to wild-type controls, however, *Nkx2.5*$^{-/-}$;*Mef2c*$^{-/-}$ mutants do not have significantly reduced cardiomyocyte volume relative to either single mutant

(Fig. 4M). Close examination of the cardiomyocytes revealed that the presumptive ventricles of *Nkx2.5*$^{-/-}$ and *Mef2c*$^{-/-}$ single mutants exhibited myocardial trabeculation (Fig. 4P, R) although the morphology of these trabeculae is overtly less robust that that of wild-type counterparts (Fig. 4N). In contrast, *Nkx2.5*$^{-/-}$;*Mef2c*$^{-/-}$ mutants showed no evidence of myocardial trabeculation (Fig. 4T, U). Indeed, the cardiomyocytes of the *Nkx2.5*$^{-/-}$;*Mef2c*$^{-/-}$ mutants (Fig. 4T, U) ostensibly resemble, in size and compaction, atrial cardiomyocytes (compare with Fig. 4O). These data indicate that *Nkx2.5*$^{-/-}$;*Mef2c*$^{-/-}$ mutant phenotypes do not represent an overt reduction in cardiomyocyte volume or size relative to either single knockout.

To molecularly characterize the single cardiac chamber seen in *Nkx2.5*$^{-/-}$;*Mef2c*$^{-/-}$ mutants we performed *in situ* hybridization upon serial sections of E9.5 embryos. *Myosin light chain 2a* (*Mlc2a*) is expressed in all early cardiomyocytes, and is thought to define the cells of the PHF and later in specific cardiomyocytes (Cai et al., 2003). *Mlc2a* expression is detected at levels comparable to those of wild-type littermates in *Nkx2.5*$^{-/-}$;*Mef2c*$^{-/-}$ mutants (Fig. 4M), confirming that PHF cardiomyocytes are specified properly in the absence of *Nkx2.5* and *Mef2c*. To further define the identify the of the single cardiac chamber seen in *Nkx2.5*$^{-/-}$;*Mef2c*$^{-/-}$ mutants, we performed *in situ* hybridization for *Mlc2v*. *In situ* hybridization analyses upon sagittal sections at E9.5 show that, as reported (Lin et al., 1997; Tanaka et al., 1999; Yamagishi et al., 2001), *Nkx2.5*$^{-/-}$ and *Mef2c*$^{-/-}$ embryos express the ventricular marker *Mlc2v* (Fig. 5H, K). However, in *Nkx2.5*$^{-/-}$;*Mef2c*$^{-/-}$ double mutant embryos, *Mlc2v* expression is not detected. These results indicate that *Nkx2.5*$^{-/-}$;*Mef2c*$^{-/-}$ double mutant embryos lack defined ventricle structures, and that differentiation of PHF cardiomyocytes is absent.

Conversely, the LIM homeodomain transcription factor *Islet1* is expressed in cells of the SHF (Cai et al., 2003). *Islet1* is robustly expressed in both wild-type and *Mef2c*$^{-/-}$ mutant embryos (Fig. 5C, F, L), although there were fewer *Islet1*-positive cells in the *Mef2c*$^{-/-}$ PAs, consistent with the previously mentioned hypoplasia (Fig. 5L). Previous studies have shown that Nkx2.5 negatively regulates *Islet1* expression (Prall et al., 2007). Consistent with this observation, *Islet1* expression is expanded into the inner curvature of the presumptive ventricle and atria of *Nkx2.5*$^{-/-}$ mutants, although an *Islet1*-negative region persists along the medial heart tube (arrow, Fig. 5I). *Islet1* is expressed uniformly across the inner curvature of the *Nkx2.5*$^{-/-}$;*Mef2c*$^{-/-}$ mutant heart (Fig. 5O). This may reflect that ectopic *Islet1*-positive cells in the OFT and atria are not separated by the developing ventricle. Alternatively, it may reflect a deficiency of SHF precursors coincident with the PA hypoplasia seen in the *Mef2c*$^{-/-}$ and *Nkx2.5*$^{-/-}$;*Mef2c*$^{-/-}$ mutants.

We thus hypothesized that this genetic interaction may reflect either that ventricular cardiomyocytes fail to be specified in the absence of *Nkx2.5* and *Mef2c*, or that ventricular cardiomyocytes are specified but are unable to proliferate and/or survive in the combined absence of both of these factors. To distinguish between these two possibilities, we examined *Mlc2v* expression in developmentally earlier *Nkx2.5*$^{-/-}$;*Mef2c*$^{-/-}$ double mutant embryos. Again, although *Mlc2v* is expressed in *Nkx2.5*$^{-/-}$ and *Mef2c*$^{-/-}$ single mutant hearts at E8.5 (Fig. 6F, J), it is absent from *Nkx2.5*$^{-/-}$;*Mef2c*$^{-/-}$ double mutant embryo hearts (Fig. 6N), while expression of *Mlc2a* is comparable to wild-type levels in all mutants examined (Fig. 6A, E, I and M). Additionally, *Myosin light chain 1v* (*Mlc1v*), which is expressed in both atrial and ventricular presumptive cardiac chambers at E8.5 (Lyons et al., 1990), is expressed, albeit at reduced levels, in *Nkx2.5*$^{-/-}$;*Mef2c*$^{-/-}$ double mutant hearts (Fig. 6O). Furthermore the expression domain of *Tbx5*, which is normally restricted to the primitive atria and left ventricle (Fig. 6D; (Bruneau et al., 1999), is expanded anteriorly in the heart tubes of *Nkx2.5*$^{-/-}$ (Fig. 6H), and *Mef2c*$^{-/-}$ (Fig. 6L; (Vong et al., 2006) mutants. This ectopic expression is also evident in *Nkx2.5*$^{-/-}$;*Mef2c*$^{-/-}$ mutants (Fig. 6P), suggesting

that the majority of cardiomyocytes within the *Nkx2.5*$^{-/-}$;*Mef2c*$^{-/-}$ double mutant heart are of atrial identity.

We further assessed cell death and cell proliferation in *Nkx2.5*$^{-/-}$;*Mef2c*$^{-/-}$ double mutant hearts. TUNEL analyses to detect cells undergoing apoptosis showed that, at E8.5 (5−11 somites), although TUNEL positive cells are detectable within the surface ectoderm (se) and foregut endoderm (fe) of wild-type, *Nkx2.5*$^{-/-}$, and *Mef2c*$^{-/-}$, and *Nkx2.5*$^{-/-}$;*Mef2c*$^{-/-}$ embryos, these cells were extremely rare in the myocardium, and no significant difference was scored between each of the various genotypes (Fig. 7A-D). Ki67 is expressed in actively proliferating cells. Immunohistochemistry using an α-Ki67 antibody shows that myocardial cells at E8.5 (5−12 somite stage) are highly proliferative (Fig. 7F-I). We quantified the number of Ki67 positive cells and expressed this number as a percentage of total cells counted. In wild-type, *Nkx2.5*$^{-/-}$, and *Mef2c*$^{-/-}$, mutants at 10−12 somite stage, after chamber specification has become apparent, Ki67 positive cells were counted solely in the atria, as molecular analyses indicate that this tissue is more comparable to the single cardiac chamber seen in *Nkx2.5*$^{-/-}$;*Mef2c*$^{-/-}$ double mutants. We saw no significant difference in cell proliferation among wild-type and mutant embryos (Fig. 7J), indicating that a loss of both *Nkx2.5* and *Mef2c* does not alter cardiomyocyte proliferation. Combined with our aforementioned morphometric data, these alterations in gene expression seen in the apparent absence of increased cardiomyocyte cell death or decreased cell proliferation suggest that *Nkx2.5* and *Mef2c* genetically interact in a manner that potentially effects ventricular cardiomyocyte specification and chamber formation.

Discussion

Here we identify molecular and genetic interactions between Nkx2.5 and Mef2c during ventricular morphogenesis. We provide evidence that Nkx2.5 and Mef2c display a novel molecular interaction through co-immunoprecipitation experiments and mammalian 2-hybrid analyses, which are reflected, *in vivo*, by functional genetic cooperative interactions. Based upon these two experimental data sets, the nature of this interaction may constitute formation of a heteromeric complex which influences respective homodimer formation. Co-immunoprecipitation data indicates that Nkx2.5 and Mef2c can directly interact with one another. Interestingly, results from mammalian 2-hybrid experiments suggest that Nkx2.5 and Mef2c interactions do not reflect stable heterodimerization, but rather formation of a complex that modulates homodimer formation, a model which is partially supported by further co-immunoprecipitation analyses. If this indeed is the mechanism by which these two factors interact, then Mef2c would enhance formation of the Nkx2.5 homodimer, while Nkx2.5 would disrupt formation of the Mef2c homodimer. These data support the idea that Mef2c monomer interactions with the Nkx2.5 homodimer result in increased stabilization and/or increased transcriptional activity. The observation that this direct Nkx2.5-Mef2c interaction is detectable in co-immunoprecipitation experiments, but not mammalian 2-hybrid assays designed to look at heterodimer formation, seems to suggest that heterodimer interactions are unstable and transient. Alternatively, the dose-dependent enhancement of Nkx2.5 homodimer formation by Mef2c could be explained by Nkx2.5-Mef2c transcriptional synergy. We feel this is far less likely if this were the case, one would expect that the synergy would also be observed while using Mef2c bait and prey and adding Nkx2.5 (Fig. 1E, G). This hypothesis suggests that Mef2c-Nkx2.5 interactions would act to remove Mef2c dimers from the cell, and, as such, would decrease relative Mef2c homodimer stability and activity whilst concurrently increasing stability of the Nkx2.5 homodimer. These novel interactions may influence specific transcriptional programs within the nascent heart, enabling the specification of distinct cardiac segments via a broadly expressed complement of transcription factors. Furthermore, they may underlie the mechanism at root of the observed genetic interaction, where *Nkx2.5* and *Mef2c*, which are broadly expressed

in nascent cardiogenic tissues (Fig. 2A, B), can synergistically coordinate ventricular cardiomyocyte development.

The pronounced genetic interaction evident in *Nkx2.5*$^{-/-}$;*Mef2c*$^{-/-}$ mutants is somewhat surprising in light of previous studies which have reported that, although *Nkx2.5* expression is unaffected in *Mef2c*$^{-/-}$ mutants (Lin et al., 1997), *Mef2c* is significantly downregulated in *Nkx2.5*$^{-/-}$ mutant hearts at E9.5 (Tanaka et al., 1999). Our *in situ* hybridization analyses revealed that, at E8.5 (7−13 somite stage), *Mef2c* is robustly expressed in *Nkx2.5*$^{-/-}$ mutant hearts (Fig. 2D). These data indicate that a loss of *Nkx2.5* may cause a gradual diminution of cardiac *Mef2c* expression, but does not affect initial *Mef2c* upregulation, and that in the early heart tube, these two genes thus occupy parallel developmental pathways. As Nkx2.5 and Mef2c are transcription factors which genetically interact, these data support that these two factors modulate each other's activity post-translationally, possibly by modifying each other's dimer potential. Our data shows that ventricular markers are absent in *Nkx2.5*$^{-/-}$;*Mef2c*$^{-/-}$ mutants, while expression of *Tbx5*, an atrial marker, persists. Additionally, we fail to detect a reduction in cardiomyocyte volume in *Nkx2.5*$^{-/-}$;*Mef2c*$^{-/-}$ embryos relative to either of the single mutants, in the absence of defects in cell death or cell proliferation. As specification of atrial identity requires an instructive signal from retinoic acid (RA), ventricular identity is considered the default cardiomyocyte identity (Heine et al., 1985; Niederreither et al., 1999; Chazaud et al., 1999; Xavier-Neto et al., 1999). The data presented here indicates that early cardiomyocyte progenitors can differentiate, but fail to assume a ventricular cell fate in the absence of both *Nkx2.5* and *Mef2c*. This seems to suggest that a ventricular identity is not the default identity for differentiating cardiomyocytes, and that differentiating cardiomyocytes require the cooperative instructive *trans*-activity of Nkx2.5 and Mef2c to adopt a ventricular cell fate. It is possible that committed PHF and SHF cardiac precursors, in the absence of Nkx2.5 and Mef2c *trans*-activity, but in the presence of RA signal, differentiate into atrial cardiomyocytes or retain a progenitor identity, respectively. Alternatively, putative ventricular cardiomyocytes may assume an intermediate identity, in which they fail to upregulate *Mlc2v* and ectopically express *Tbx5*. A third possible mechanism for the loss of the ventricle could be that Nkx2.5 and Mef2c are uniquely essential in distinct and complementary populations of ventricular progenitors within, for example, the PHF and SHF, and that the cumulative loss of these cell populations by disruption of both *Nkx2.5* and *Mef2c* causes complete ventricular hypoplasia. Disruption of *Nkx2.5* leads to impaired SHF cell addition to the ventricle (Prall et al., 2007), while *Mef2c*$^{-/-}$ mutant SHF cells, while not as extensively studied, do contribute to the developing ventricle (Verzi et al., 2005). Rather, aberrant contribution of PHF cells to the atrium instead of the ventricle initially causes the reduced ventricle characteristic of *Mef2c*$^{-/-}$ mutants (Vong et al., 2006). Thus, the ventricular hypoplasia seen in *Nkx2.5*$^{-/-}$;*Mef2c*$^{-/-}$ embryos may reflect the cumulative unique requirements of Nkx2.5 and Mef2c for SHF and PHF-derived ventricular cell differentiation, respectively. Further studies are warranted to distinguish between these three possibilities. Additional molecular and electro-physiological marker analyses would confirm the *Tbx5*-expressing cells as atrial. Utilization of conditional alleles of *Mef2c* (Vong et al., 2005; Arnold et al., 2007) and *Nkx2.5* in combination with, for example, the α*MHC-Cre* driver (Oka et al., 2006), to ablate gene function after cardiomyocyte cell fate has been specified would enable gene expression studies to determine whether *Tbx5* expression is disregulated in committed ventricular cardiomyocytes when *Nkx2.5* and *Mef2c* function is lost. Utilization of SHF-specific *Cre* drivers, such as the *Isl1-Cre* (Srinivas et al., 2001; Cai et al., 2003), would enable confirmation that *Mef2c* and *Nkx2.5* genetically interact specifically within SHF cells. Nonetheless, our data does provide evidence that *Nkx2.5* and *Mef2c* act cooperatively to regulate the ventricular cardiomyocyte specification program.

The ventricular digenesis phenotypes of *Nkx2.5*$^{-/-}$;*Mef2c*$^{-/-}$ mice are reminiscent of phenotypes associated with *Nkx2.5*$^{-/-}$;*Hand2*$^{-/-}$ double mutant embryos (Yamagishi et al., 2001). In these mice ventricular development was also significantly curtailed, although these defects seem to represent a failure of ventricular chamber expansion, rather than differentiation. Interestingly, it has been reported that Mef2c and Hand2 can interact (Zang et al., 2004). Indeed, *Mef2c* lies upstream of *Hand2*, although *Hand2* is expressed normally within the heart tube prior to looping (Lin et al., 1997). It would be of interest to incorporate Hand2 into the biochemical studies detailed here, to assess further potential heterogenic interactions and establishment of left vs. right ventricular cardiomyocyte identity.

Given the nature of the genetic interaction presented here, it would be of interest to attempt to identify genes specifically expressed within the ventricular lineage that direct cooperative targets of Nkx2.5 and Mef2c *trans*-activity. Identification of these putative transcriptional targets would enable further studies to more deeply explore the mechanism and physiological significance of this biochemical interaction between Nkx2.5 and Mef2c.

Experimental Procedures

Mouse strains

The targeting and PCR-based genotyping strategies for the *Mef2c*^{tm1Eno} and *Nkx2.5*^{tm1Rph} null alleles have been previously described (Lyons et al., 1995; Lin et al., 1997). *Mef2c*^{tm1Eno} (hereafter called ***Mef2c***$^{-/-}$) and *Nkx2.5*^{tm1Rph} (hereafter called ***Nkx2.5***$^{+/-}$) mutant mice were maintained on a mixed (C57Bl/6−129/Sv) genetic background. Noon of the day of the vaginal plug was considered E0.5.

Histology

Embryos (E9.5 – E11.5) were fixed in 4% paraformaldehyde, dehydrated through a methanol gradient and embedded in paraffin. Embryos were sectioned at 10μm unless otherwise noted. Hematoxylin and Eosin (H&E) staining was performed exactly as described (Conway et al., 2000). Propidium iodide (PI) staining was performed using 50mg/mL PI in 2X SSC. A minimum of 2 viable embryos per genotype (assayed via the presence of a heart beat) was used for these and all subsequent analyses.

Morphometric analyses

Adobe Photoshop was used to isolate the heart in photographs of every third sagittal embryo section. Using ImageJ, photographs were converted to 8-bit grayscale/binary format. To account for variations in total heart size due to hearts being in ether systole or diastole when fixed only the area of the OFT, ventricular and atrial cardiomyocytes, not that of the cardiac lumen or sinus venosus, was measured. Total cardiomyocyte area was quantified using the Analyze Particles command. Mutant cardiomyocyte areas were expressed as a percentage relative to somite-matched wild-type controls. Significance was determined using a students two-tailed T-test assuming equal variances.

TUNEL and Immunohistochemistry

TUNEL assays were performed using Apoptag Cell Death Detection Kit (Chemicon) as per manufacturer's instruction. For immunohistochemistry, heat-induced epitope retrieval was performed, in which slides were incubated in preheated 10mM sodium citrate (pH 6.0) in a 90°C water bath for 15 minutes. The heat source was subsequently removed, and the slides allowed to cool to room temperature for 1 hour. Samples were further pretreated with Avidin D and Biotin blocking solutions (Vector Laboratories) as per manufacturer's instructions. α-Ki67 monoclonal antibody (DakoCytomation) was used at 1:500 dilution in combination

with a Rabbit a-Rat IgG (Vector Laboratories) diluted 1:250 and SA-Fluorescein (Vector Laboratories) diluted 1:200.

In situ hybridization

Digoxygenin labeled section *in situ* hybridizations were carried out using established protocols on 10μm paraffin sections (Nagy, 2003; Chen et al., 2004) using T7, T3 or SP6 polymerases (Promega) and DIG-Labeling Mix (Roche). Sense and antisense digoxygenin-labeled riboprobes were transcribed for *Mlc2a*, *Mlc1v*, *Mlc2v*, *Tbx5*, and *Islet1*. Specific staining patterns for each probe were assessed in at least 3-serial sections.

Plasmid Constructs

pCS2+ was modified via addition of a FLAG epitope tag 5' of the MCS (pCS2+FLAG). PCR subcloning was used to flank *Mef2c* with XhoI sites and *Nkx2.5* with SalI sites. Each cDNA was subsequently cloned into the XhoI site of pCS2+FLAG and pCS2+MT. PCR subcloning was also used to flank *Mef2c* with a 5' BamHI site and a 3' XhoI site and *Nkx2.5* with a 5' BamHI site and a 3' SalI site. These sites were then utilized to clone each cDNA into pACT (prey vector) and pBIND (bait vector; Promega) to generate C-terminal GAL4 and VP16 fusion proteins. The pcDNA1-Mef2c and pcDNA1-Nkx2.5 expression constructs were obtained from E. Olson (UTSW). In each experiment, corresponding empty vectors were included as controls.

Mammalian two-hybrid assays

Mammalian two-hybrid assays were performed as previously reported (Firulli et al., 2000) using the dual luciferase assay kit (Promega) according to the manufacturer's protocol. Luciferase and renilla activities were read using a 96-well microtiter plate luminometer (Thermo Labsystems). Mammalian two-hybrid assays were repeated six times. Dosage curve two-hybrid assays were repeated three times.

Immunoblotting and co-immunoprecipitation experiments

HEK293 cells were transiently transfected using calcium phosphate techniques. Cells were actively lysed 48 hours after transfection with 20mM NaCl, 150mM $MgCl_2$, 2mM NP-40, 0.10% Glycerol, 10% Sodium Fluoride, 10mM Sodium Orthovanadate, 0.1mM Sodium Pyrophosphate and 10mM DTT plus protease inhibitors, and incubated with αFLAG monoclonal antibody M2 conjugated beads (Sigma) for 2 hours. Samples were washed three times in PBS, boiled in loading dye, run through a 10% SDS PAGE and visualized utilizing horseradish peroxidase-conjugated α-mouse immunoglobulin (Ig)G antibody and ECL detection kit (Amersham Pharmacia Biotech). Co-IPs were preformed at least 3 times with similar results.

Acknowledgments

We would like to thank members of the Firulli and Conway labs for technical assistance. We would also like to thank the Riley Heart Research Center for helpful input during group discussions. Infrastructural support at the Herman B Wells Center for Pediatric Research is in part supported by the generosity of the Riley Children's Foundation and Division of Pediatric Cardiology. This work is supported by the NIH RO1HL061677-09 (ABF), NIH NCI T32CA111198 (JWV) and NIH 1P01HL085098-01A1 (ABF & SJC).

Literature Cited

Arnold MA, Kim Y, Czubryt MP, Phan D, McAnally J, Qi X, Shelton JM, Richardson JA, Bassel-Duby R, Olson EN. MEF2C transcription factor controls chondrocyte hypertrophy and bone development. Dev Cell. 2007; 12:377–389. [PubMed: 17336904]

Bruneau BG, Logan M, Davis N, Levi T, Tabin CJ, Seidman JG, Seidman CE. Chamber-specific cardiac expression of Tbx5 and heart defects in Holt-Oram syndrome. Dev Biol. 1999; 211:100–108. [PubMed: 10373308]

Cai CL, Liang X, Shi Y, Chu PH, Pfaff SL, Chen J, Evans S. Isl1 identifies a cardiac progenitor population that proliferates prior to differentiation and contributes a majority of cells to the heart. Dev Cell. 2003; 5:877–889. [PubMed: 14667410]

Chen CM, Chang JL, Behringer RR. Tumor formation in p53 mutant ovaries transplanted into wild-type female hosts. Oncogene. 2004; 23:7722–7725. [PubMed: 15334065]

Conway SJ, Bundy J, Chen J, Dickman E, Rogers R, Will BM. Decreased neural crest stem cell expansion is responsible for the conotruncal heart defects within the splotch (Sp(2H))/Pax3 mouse mutant. Cardiovasc Res. 2000; 47:314–328. [PubMed: 10946068]

Durocher D, Charron F, Warren R, Schwartz RJ, Nemer M. The cardiac transcription factors Nkx2−5 and GATA-4 are mutual cofactors. Embo J. 1997; 16:5687–5696. [PubMed: 9312027]

Durocher D, Chen CY, Ardati A, Schwartz RJ, Nemer M. The atrial natriuretic factor promoter is a downstream target for Nkx-2.5 in the myocardium. Mol Cell Biol. 1996; 16:4648–4655. [PubMed: 8756621]

Edmondson DG, Lyons GE, Martin JF, Olson EN. Mef2 gene expression marks the cardiac and skeletal muscle lineages during mouse embryogenesis. Development. 1994; 120:1251–1263. [PubMed: 8026334]

Firulli AB, Thattaliyath BD. Transcription factors in cardiogenesis: the combinations that unlock the mysteries of the heart. Int Rev Cytol. 2002; 214:1–62. [PubMed: 11893163]

Firulli BA, Hadzic DB, McDaid JR, Firulli AB. The basic helix-loop-helix transcription factors dHAND and eHAND exhibit dimerization characteristics that suggest complex regulation of function. J Biol Chem. 2000; 275:33567–33573. [PubMed: 10924525]

Kasahara H, Usheva A, Ueyama T, Aoki H, Horikoshi N, Izumo S. Characterization of homo- and heterodimerization of cardiac Csx/Nkx2.5 homeoprotein. J Biol Chem. 2001; 276:4570–4580. [PubMed: 11042197]

Kelly RG, Brown NA, Buckingham ME. The arterial pole of the mouse heart forms from Fgf10-expressing cells in pharyngeal mesoderm. Dev Cell. 2001; 1:435–440. [PubMed: 11702954]

Komuro I, Izumo S. Csx: a murine homeobox-containing gene specifically expressed in the developing heart. Proc Natl Acad Sci U S A. 1993; 90:8145–8149. [PubMed: 7690144]

Lin Q, Schwarz J, Bucana C, Olson EN. Control of mouse cardiac morphogenesis and myogenesis by transcription factor MEF2C. Science. 1997; 276:1404–1407. [PubMed: 9162005]

Lints TJ, Parsons LM, Hartley L, Lyons I, Harvey RP. Nkx-2.5: a novel murine homeobox gene expressed in early heart progenitor cells and their myogenic descendants. Development. 1993; 119:969. [PubMed: 7910553]

Lyons GE, Schiaffino S, Sassoon D, Barton P, Buckingham M. Developmental regulation of myosin gene expression in mouse cardiac muscle. J Cell Biol. 1990; 111:2427–2436. [PubMed: 2277065]

Lyons I, Parsons LM, Hartley L, Li R, Andrews JE, Robb L, Harvey RP. Myogenic and morphogenetic defects in the heart tubes of murine embryos lacking the homeo box gene Nkx2−5. Genes Dev. 1995; 9:1654–1666. [PubMed: 7628699]

Mjaatvedt CH, Nakaoka T, Moreno-Rodriguez R, Norris RA, Kern MJ, Eisenberg CA, Turner D, Markwald RR. The outflow tract of the heart is recruited from a novel heart-forming field. Dev Biol. 2001; 238:97–109. [PubMed: 11783996]

Molkentin JD, Black BL, Martin JF, Olson EN. Mutational analysis of the DNA binding, dimerization, and transcriptional activation domains of MEF2C. Mol Cell Biol. 1996; 16:2627–2636. [PubMed: 8649370]

Morin S, Charron F, Robitaille L, Nemer M. GATA-dependent recruitment of MEF2 proteins to target promoters. Embo J. 2000; 19:2046–2055. [PubMed: 10790371]

Nagy, A. Manipulating the mouse embryo : a laboratory manual. Vol. x. Cold Spring Harbor Laboratory Press.; Cold Spring Harbor, N.Y.: 2003. p. 764

Oka T, Maillet M, Watt AJ, Schwartz RJ, Aronow BJ, Duncan SA, Molkentin JD. Cardiac-specific deletion of Gata4 reveals its requirement for hypertrophy, compensation, and myocyte viability. Circ Res. 2006; 98:837–845. [PubMed: 16514068]

Prall OW, Menon MK, Solloway MJ, Watanabe Y, Zaffran S, Bajolle F, Biben C, McBride JJ, Robertson BR, Chaulet H, Stennard FA, Wise N, Schaft D, Wolstein O, Furtado MB, Shiratori H, Chien KR, Hamada H, Black BL, Saga Y, Robertson EJ, Buckingham ME, Harvey RP. An Nkx2−5/Bmp2/Smad1 negative feedback loop controls heart progenitor specification and proliferation. Cell. 2007; 128:947–959. [PubMed: 17350578]

Skerjanc IS, Petropoulos H, Ridgeway AG, Wilton S. Myocyte enhancer factor 2C and Nkx2−5 up-regulate each other's expression and initiate cardiomyogenesis in P19 cells. J Biol Chem. 1998; 273:34904–34910. [PubMed: 9857019]

Srinivas S, Watanabe T, Lin CS, William CM, Tanabe Y, Jessell TM, Costantini F. Cre reporter strains produced by targeted insertion of EYFP and ECFP into the ROSA26 locus. BMC Dev Biol. 2001; 1:4. [PubMed: 11299042]

Srivastava D. Genetic assembly of the heart: implications for congenital heart disease. Annu Rev Physiol. 2001; 63:451–469. [PubMed: 11181963]

Sucov HM. Molecular insights into cardiac development. Annu Rev Physiol. 1998; 60:287–308. [PubMed: 9558465]

Tanaka M, Chen Z, Bartunkova S, Yamasaki N, Izumo S. The cardiac homeobox gene Csx/Nkx2.5 lies genetically upstream of multiple genes essential for heart development. Development. 1999; 126:1269–1280. [PubMed: 10021345]

Vanpoucke G, Goossens S, De Craene B, Gilbert B, van Roy F, Berx G. GATA-4 and MEF2C transcription factors control the tissue-specific expression of the alphaT-catenin gene CTNNA3. Nucleic Acids Res. 2004; 32:4155–4165. [PubMed: 15302915]

Verzi MP, McCulley DJ, De Val S, Dodou E, Black BL. The right ventricle, outflow tract, and ventricular septum comprise a restricted expression domain within the secondary/anterior heart field. Dev Biol. 2005; 287:134–145. [PubMed: 16188249]

Vong L, Bi W, O'Connor-Halligan KE, Li C, Cserjesi P, Schwarz JJ. MEF2C is required for the normal allocation of cells between the ventricular and sinoatrial precursors of the primary heart field. Dev Dyn. 2006; 235:1809–1821. [PubMed: 16680724]

Vong LH, Ragusa MJ, Schwarz JJ. Generation of conditional Mef2cloxP/loxP mice for temporal- and tissue-specific analyses. Genesis. 2005; 43:43–48. [PubMed: 16106363]

Waldo KL, Kumiski DH, Wallis KT, Stadt HA, Hutson MR, Platt DH, Kirby ML. Conotruncal myocardium arises from a secondary heart field. Development. 2001; 128:3179–3188. [PubMed: 11688566]

Yamagishi H, Yamagishi C, Nakagawa O, Harvey RP, Olson EN, Srivastava D. The combinatorial activities of Nkx2.5 and dHAND are essential for cardiac ventricle formation. Dev Biol. 2001; 239:190–203. [PubMed: 11784028]

Zang MX, Li Y, Xue LX, Jia HT, Jing H. Cooperative activation of atrial naturetic peptide promoter by dHAND and MEF2C. J Cell Biochem. 2004; 93:1255–1266. [PubMed: 15486975]

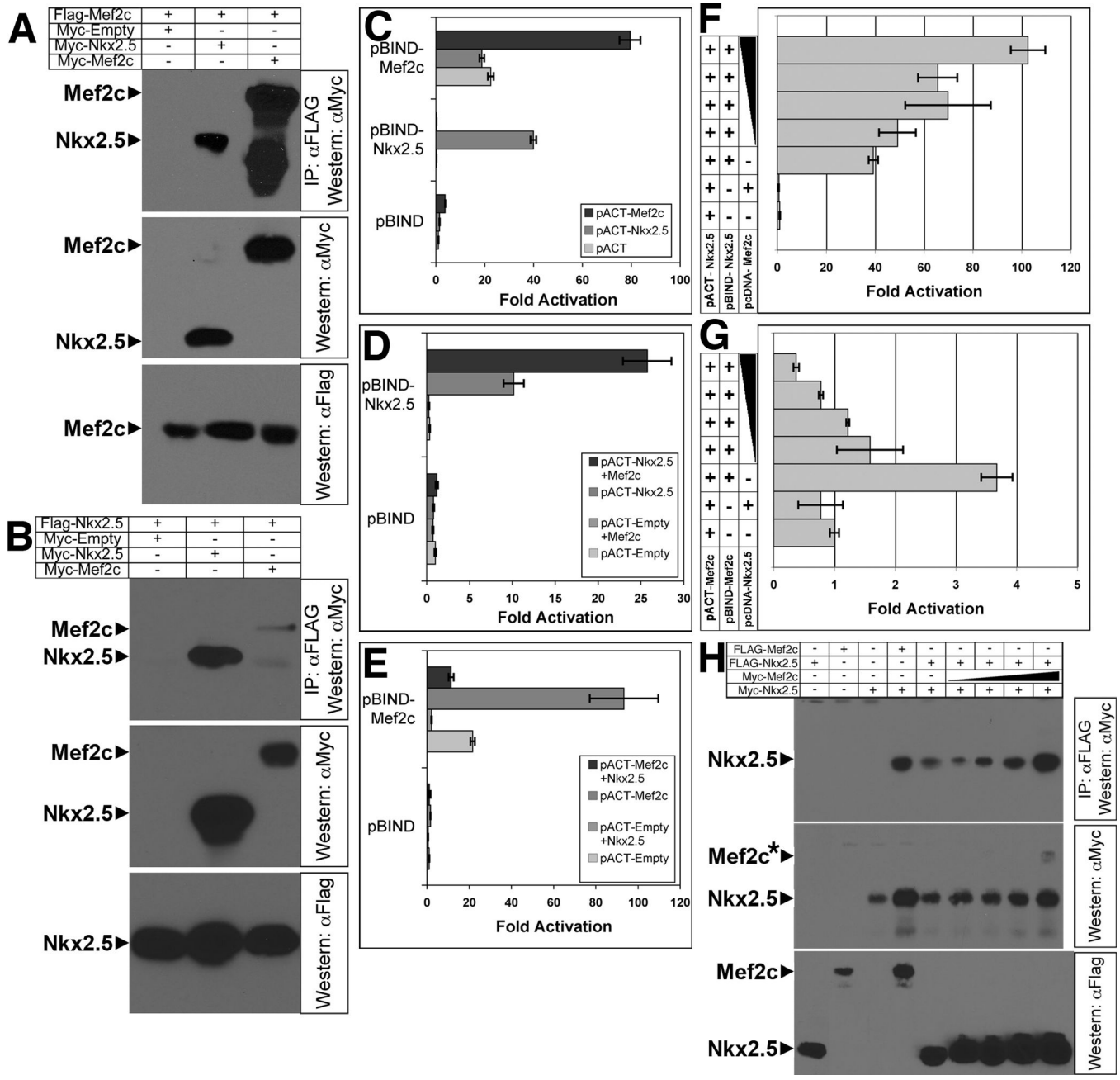

Figure 1. Physical interaction between *Nkx2.5* and *Mef2c*

A) Myc-Nkx2.5 and Myc-Mef2c coexpressed in HEK293 cells and immunoprecipitated with FLAG-Mef2c. Note that a smaller migrating form of Myc-Mef2c is observed, likely reflecting some protein degradation. B) Myc-Nkx2.5 and Myc-Mef2c coexpressed in HEK293 cells and immunoprecipitated with FLAG-Nkx2.5. C-E) Mammalian 2-hybrid assays assessing protein-protein interactions between Nkx2.5 and Mef2c (C, n=6), enhancement of Nkx2.5 protein-protein interactions by the addition of Mef2c (D, n=6), disruption of Mef2c protein-protein interactions by coexpression of Nkx2.5 (E, n=6), and dose dependence of Mef2c and Nkx2.5 homodimerization upon respective coexpressed levels of Nkx2.5 or Mef2c (F, G, n=3). H) Myc-Nkx2.5 and Myc-Mef2c coexpressed in HEK293 cells and immunoprecipitated with FLAG-Nkx2.5, showing greater precipitation of

Nkx2.5 in the presence of increasing levels of Mef2c. * Due to a relatively low level of expression, in the Western blot showing total Myc-tagged protein, the Myc-Mef2c gradient is not detectable at lower concentrations. In A, B, H and I, the upper blot shows αMyc immunoblot of αFLAG precipitation, and the lower two blots show total Myc- and FLAG-tagged protein.

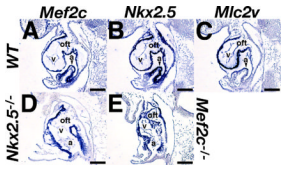

Figure 2. Expression of *Nkx2.5* and *Mef2c* in wild-type and mutant hearts at E8.5

DIG-labeled *in situ* hybridization upon serial sagittal sections of 9 somite stage embryos showing *Mef2c* (A, D), *Nkx2.5* (B, C) and *Mlc2v* (C) in the hearts of wild-type (A-C), *Nkx2.5*$^{-/-}$ (D) and *Mef2c*$^{-/-}$ (E) embryos, a; oft, outflow tract; v, ventricle.

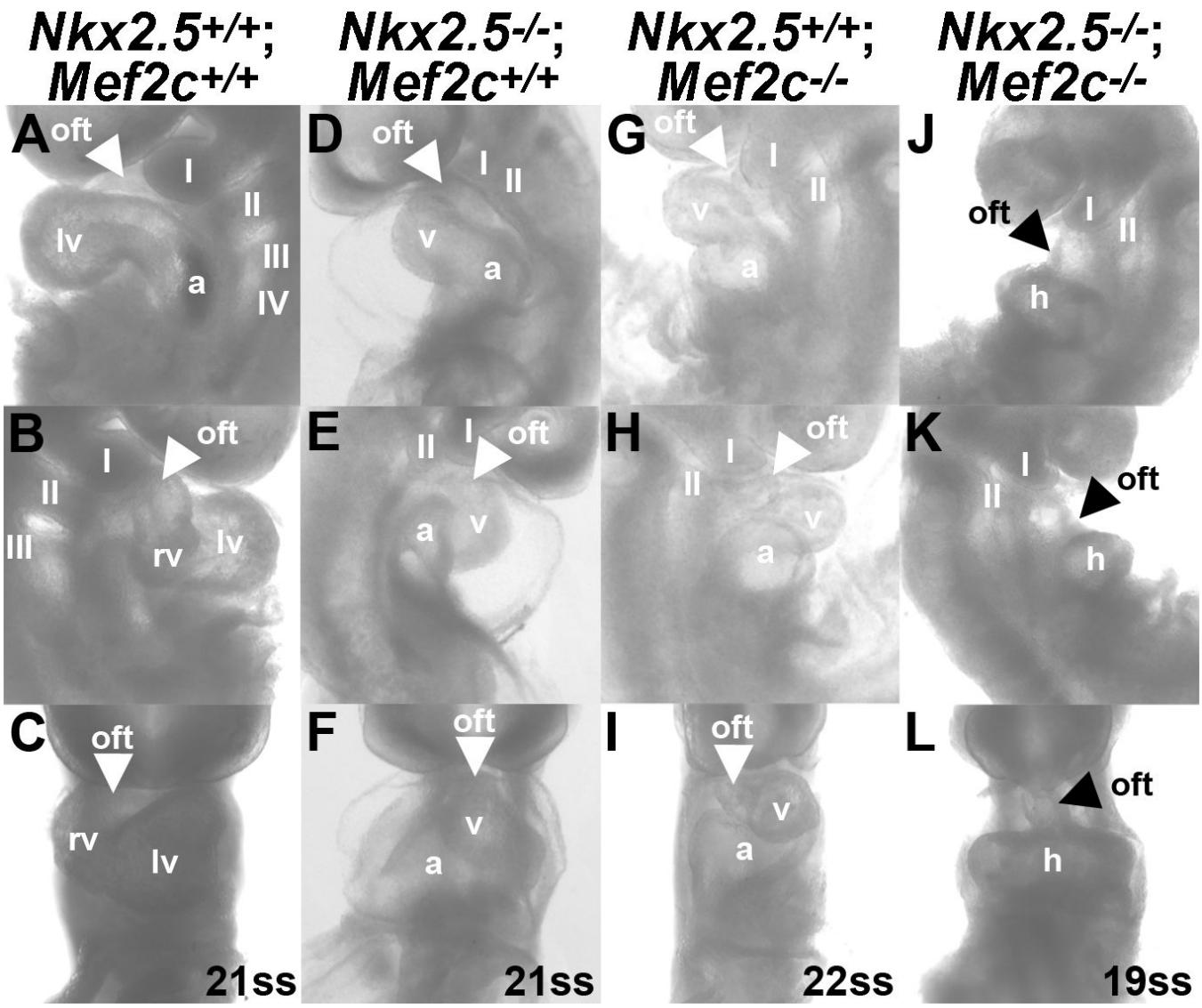

Figure 3. Molecular marker analysis of genetic cooperation between *Nkx2.5* and *Mef2c*

Whole mount preparations of E9.5 wild-type (A-C), *Nkx2.5*$^{-/-}$ (D-F), *Mef2c*$^{-/-}$ (G-I) and *Nkx2.5*$^{-/-}$;*Mef2c*$^{-/-}$ (J-L) embryos shown in right (A, D, G, J) and left lateral (B, E, H, K) and frontal (C, F, I, L) views. Arrowheads denote the outflow tract. Roman numerals denote first through fourth pharyngeal arches. a, atria; h, heart; lv, left ventricle; oft, outflow tract; rv, right ventricle; v, ventricle; ss, somite stage.

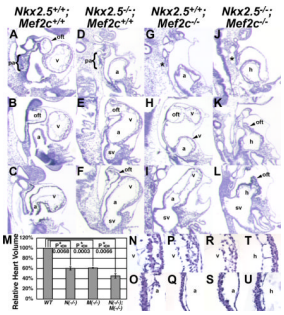

Figure 4. Histological analyses of functional genetic cooperation between *Nkx2.5* and *Mef2c*

A-L) H&E stained sagittal sections of E9.5 wild-type (A-C), *Nkx2.5*$^{-/-}$ (D-F), *Mef2c*$^{-/-}$ (G-I) and *Nkx2.5*$^{-/-}$;*Mef2c*$^{-/-}$ (J-L) embryos. Asterisks denote absence of caudal pharyngeal arches. M) Morphometric comparisons of cardiomyocyte area in wild-type (*WT*), *Nkx2.5*$^{-/-}$ (*N(−/−)*), *Mef2c*$^{-/-}$ (*M(−/−)*) and *Nkx2.5*$^{-/-}$;*Mef2c*$^{-/-}$ (*N(−/−)*;*M(−/−)*) embryos at E9.5. Cardiomyocyte area from serial sections of E9.5 embryos was quantitated using ImageJ software. All three mutant genotypes assayed showed significantly diminished cardiomyocyte volume, however, *Nkx2.5*$^{-/-}$;*Mef2c*$^{-/-}$ hearts did not have significantly smaller hearts relative to either single mutant. N-U) High-magnification images of H&E stained sagittal sections of E9.5 embryos comparing *Nkx2.5*$^{-/-}$;*Mef2c*$^{-/-}$ (T, U) mutant cardiomyocytes against ventricular (N, P, and R) and atrial (O, Q, and S) cardiomyocytes from wild-type (N, O), *Nkx2.5*$^{-/-}$ (P, Q) and *Mef2c*$^{-/-}$ (R, S) embryos. a, atria; h, heart chamber; oft, outflow tract; pa, pharyngeal arches; sv, sinus venosus; v, ventricle.

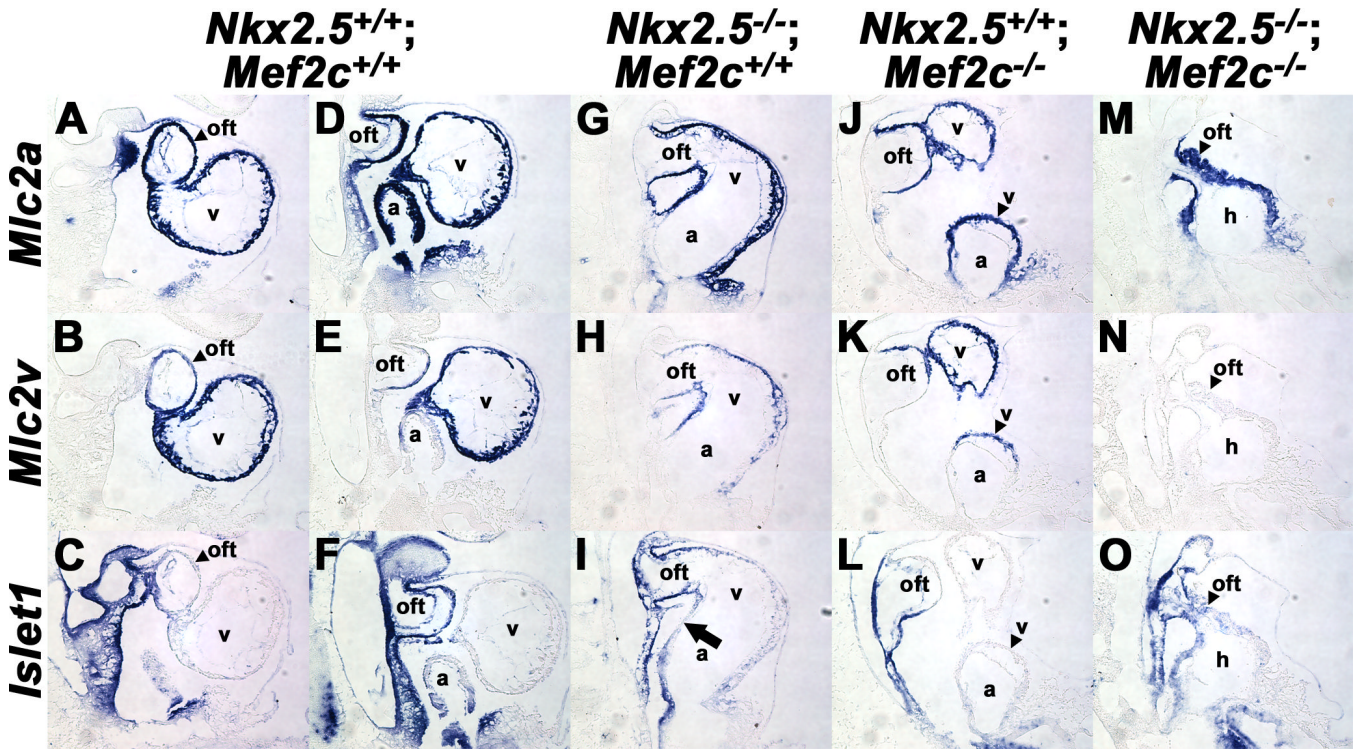

Figure 5. Molecular analyses of cardiomyocyte differentiation within *Nkx2.5* and *Mef2c* mutant hearts

DIG-labeled *in situ* hybridization upon serial sagittal sections of 20−22 somite stage embryos showing *Mlc2a* (A, D, G, J, M), *Mlc2v* (B, E, H, K, N) and *Islet1* (C, F, I, L, O) expression in the hearts of wild-type (A-F), *Nkx2.5*$^{-/-}$ (G-I), *Mef2c*$^{-/-}$ (J-L) and *Nkx2.5*$^{-/-}$;*Mef2c*$^{-/-}$ (M-O) embryos. Arrow denotes *Islet1* negative region within the inner curvature of the *Nkx2.5*$^{-/-}$ heart. a, atria; h, heart chamber; oft, outflow tract; pa, pharyngeal arches; sv, sinus venosus; v, ventricle.

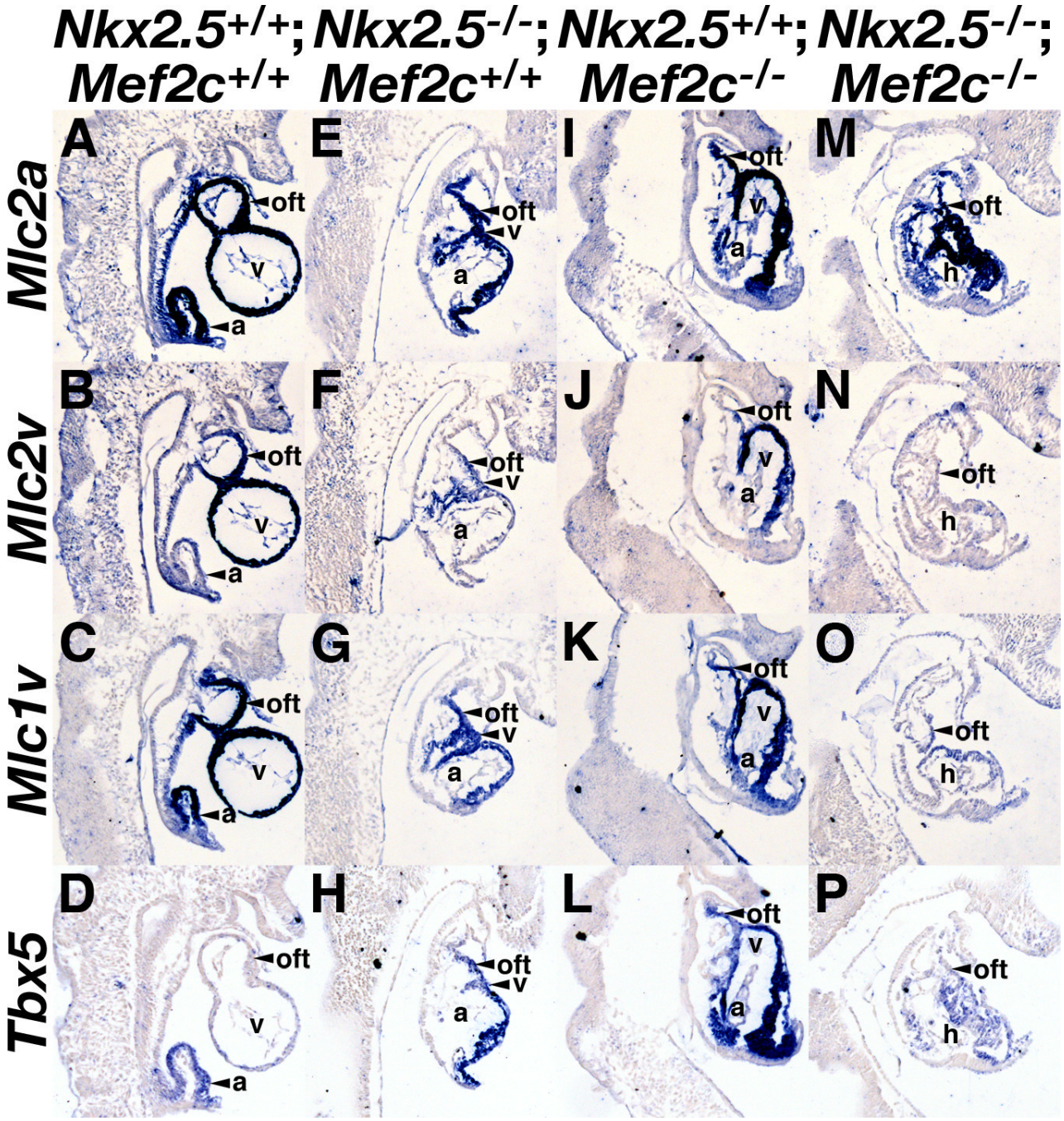

Figure 6. Molecular analyses of cardiomyocyte specification within *Nkx2.5* and *Mef2c* mutants

DIG-labeled *in situ* hybridization upon serial sagittal sections of 10 somite stage embryos showing *Mlc2a* (A, E, I, M), *Mlc2v* (B, F, J, N), *Mlc1v* (C, G, K, O), and *Tbx5* (D, H, L, P) expression in the hearts of somite-matched wild-type (A-D), *Nkx2.5*$^{-/-}$ (E-H), *Mef2c*$^{-/-}$ (I-L) and *Nkx2.5*$^{-/-}$;*Mef2c*$^{-/-}$ (M-P) embryos. a, atria; h, heart chamber; oft, outflow tract; v, ventricle.

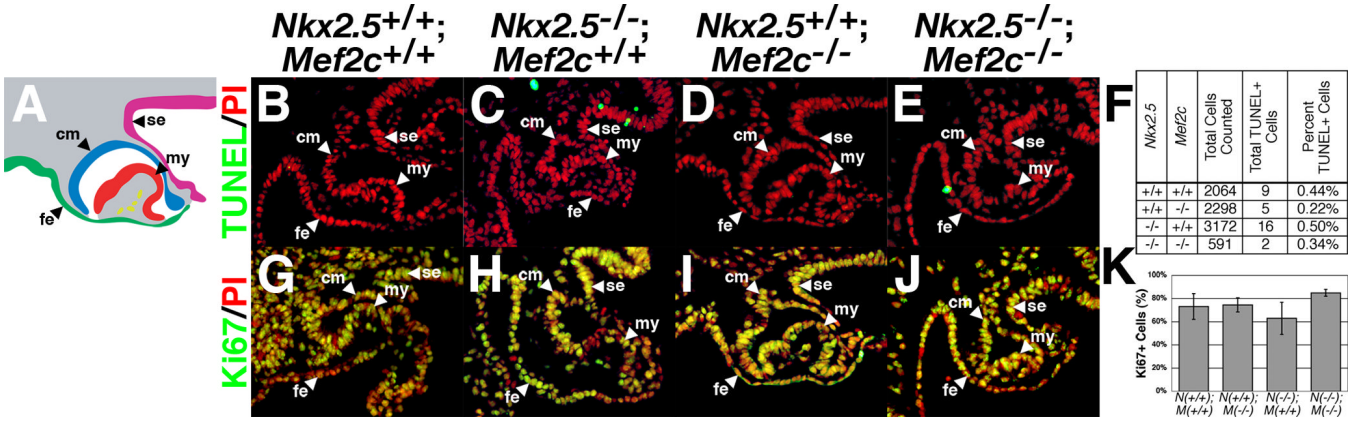

Figure 7. Cell death and cell proliferation in embryos lacking *Nkx2.5* and/or *Mef2c*

A) Schematic representation of the structures depicted in (B-E) and (G-J) included for ease of interpretation. B-E) TUNEL staining of 5−7 somite stage embryos show that TUNEL-positive cells (green) are seen within the surface ectoderm and foregut endoderm, but are rarely detectable in the myocardium of wild-type (B), *Nkx2.5*$^{-/-}$ (C), *Mef2c*$^{-/-}$ (D) or *Nkx2.5*$^{-/-}$;*Mef2c*$^{-/-}$ (E) embryos. Quantitated numbers of apoptotic cells observed are summarized in (F). G-J) αKi67 antibody staining upon sagittal sections of the same embryos reveals that the nascent myocardium is highly proliferative in all genotypes examined. The percentage of Ki67 positive cells in cardiomyocytes of embryos from 5−12 somites is quantified in (K). Sections are counterstained with propidium iodide (PI; red). ce, coelemic mesothelium (blue); endocardium (yellow); fe, foregut endoderm (green); my, myocardium (red); se, surface ectoderm (violet).